ISSN 1674-1056
http://cpb.iphy.ac.cn
http://iopscience.iop.org/cpb
中国物理 B
Chinese Physics
中国物理
Chinese Physics B

Ferromagnetism and magnetostructural coupling in V-doped MnNiGe alloys

Hui Yang, Jun Liu, Chao Li, Guang-Long Wang, Yuan-Yuan Gong, Feng Xu

Citation: Chin. Phys. B. 2018, 27 (**10**): 107502 **doi:** 10.1088/1674-1056/27/10/107502

Journal homepage: http://cpb.iphy.ac.cn; http://iopscience.iop.org/cpb

What follows is a list of articles you may be interested in

Progress of novel diluted ferromagnetic semiconductors with decoupled spin and charge doping: Counterparts of Fe-based superconductors

Shengli Guo(郭胜利), Fanlong Ning(宁凡龙)

Chin. Phys. B . 2018, 27(9): 097502. **doi:** 10.1088/1674-1056/27/9/097502

Magnetic properties of AlN monolayer doped with group 1A or 2A nonmagnetic element: First-principles study

Ruilin Han(韩瑞林), Xiaoyang Chen(陈晓阳), Yu Yan(闫羽)

Chin. Phys. B . 2017, 26(9): 097503. **doi:** 10.1088/1674-1056/26/9/097503

Influence of Ni/Mn ratio on magnetostructural transformation and magnetocaloric effect in $Ni_{48-x}Co_2Mn_{38+x}Sn_{12}$ (x = 0, 1.0, 1.5, 2.0, and 2.5) ferromagnetic shape memory alloys

Ishfaq Ahmad Shah, Najam ul Hassan, Abdur Rauf, Jun Liu(刘俊), Yuanyuan Gong(龚元元), Guizhou Xu(徐桂舟), Feng Xu(徐锋)

Chin. Phys. B . 2017, 26(9): 097501. **doi:** 10.1088/1674-1056/26/9/097501

Effects of Zr substitution on structural, morphological, and magnetic properties of bismuth iron oxide phases

A Asif, M Hassan, S Riaz, S Naseem, S S Hussain

Chin. Phys. B . 2017, 26(8): 087502. **doi:** 10.1088/1674-1056/26/8/087502

Electronic structures and magnetic properties of Zn- and Cd-doped AlN nanosheets: A first-principles study

Rui-Lin Han(韩瑞林), Shi-Min Jiang(姜世民), Yu Yan(闫羽)

Chin. Phys. B . 2017, 26(2): 027502. **doi:** 10.1088/1674-1056/26/2/027502

Ferromagnetism and magnetostructural coupling in V-doped MnNiGe alloys*

Hui Yang(杨慧), Jun Liu(刘俊), Chao Li(李超), Guang-Long Wang(王广龙), Yuan-Yuan Gong(龚元元), and Feng Xu(徐锋)†

MIIT Key Laboratory of Advanced Metallic and Intermetallic Materials Technology, School of Materials Science and Engineering, Nanjing University of Science and Technology, Nanjing 210094, *China.*

(Received 21 July 2018; revised manuscript received 16 August 2018; published online 27 September 2018)

The magnetostructural coupling between magnetic and structure transitions plays an important role in the multifunctional applications of magentocaloric materials. In this work, ferromagnetism and magnetostructural transformation are achieved in nonmagnetic V-doped MnNiGe alloys. With simultaneously reducing the transformation temperature and converting antiferromagnetic martensite to ferromagnetic state, the magnetostructural transformation between ferromagnetic orthorhombic phase and paramagnetic hexagonal phase is established in a temperature region as large as 130 K. The magnetic-field-induced magnetostructural transformation is accompanied by considerable magnetocaloric effect.

Keywords: magnetostructural transformation, ferromagnetism, magnetocaloric effect

PACS: 75.30.Kz, 75.30.Sg, 75.50.Gg, 75.60.Ej **DOI:** 10.1088/1674-1056/27/10/107502

1. Introduction

Magnetostructural transformation (MST), a coinciding magnetic and crystallographic transition, has attracted great attention for its multimagnetoresponsive effects, such as magnetic shape memory effect,[1] exchange bias effect,[2] magnetoresistance[3,4] magnetic field-induced strain[5] and large magnetocaloric effect (MCE).[6,7] Recently, it has been found that MnMX-based alloys, where M is Co or Ni and X is nonmagnetic *sp* element Si or Ge,[8] exhibit a thermo-induced structural transformation between high-temperature hexagonal and low-temperature orthorhombic phase. On condition that the transformation temperature (T_t) is tuned into a temperature region between the Curie-temperatures of the two phases ($T_{C,H}$ and $T_{C,O}$, the subscripts H and O correspond to the hexagonal and orthorhombic phases, respectively.), MST between paramagnetic (PM) hexagonal and ferromagnetic (FM) orthorhombic phases can be achieved.[9] The accompanied large magnetization difference (ΔM) is favorable for the magnetic-field-induced MST, resulting in large magnetic entropy change (ΔS_m).[10] The obtained ΔS_m is comparable to those of some famous magnetocaloric materials,[11] indicating the potential applications in magnetic cooling refrigerator.

In MnMX family, MnNiGe alloy is a special member since the hexagonal MnNiGe is a ferromagnet with $T_{C,H} \sim 205$ K, while the orthorhombic one is spiral antiferromagnetic (AFM) below its Néel temperature ~ 346 K.[12] On the premise that the magnetic state of orthorhombic phase keeps unchanged, the only way to fulfill an MST with large ΔM is to reduce the T_t to a value lower than $T_{C,H}$ and thus the MST between AFM orthorhombic and FM hexagonal phase can be obtained.[1,13,14] Although this AFM–FM MST can be induced by the magnetic field, there exist two accompanying disadvantages. One is the low-temperature MST as well as the associated physical effect, which is not convenient to the potential utilization at ambient temperature.[15] The other is the narrow temperature region, in which the MST can be fulfilled, because it is reported that the MST will soon disappear once the T_t is below $T_{C,H}$.[16]

The promising way to solve the two disadvantages is to change the ground magnetic state of orthorhombic phase from AFM to FM. In that case, the MST can be established between PM hexagonal and FM orthorhombic phase in a temperature range from $T_{C,H}$ to $T_{C,O}$.[16] This temperature region is as large as 141 K and also covers room temperature. As reported before, the magnetic state of orthorhombic phase is sensitive to the atomic environment and the introduction of magnetic element Fe or Co can efficiently change its magnetic state into FM state.[17,18] In this work, we will use a nonmagnetic element V to activate the FM coupling in orthorhombic phase. Simultaneously, the V-doping also reduces the T_t, and thus leading to PM-FM MST. Based on this improvement, large MCE is achieved in this V-doped MnNiGe alloy.

2. Experiment details

Polycrystalline samples with compositions of $MnNi_{1-x}V_xGe$ ($x = 0.10$, 0.12, 0.14, 0.16, and 0.18) were prepared by arc melting high-purity metals in argon atmosphere. The ingots were then sealed in a vacuum quartz tube and annealed at 1123 K for 72 h followed by rapid quenching in ice water. The structure data were obtained using a

*Project supported by the Key Research & Development Program of Jiangsu Province, China (Grant No. BE2017102)

†Corresponding author. E-mail: xufeng@njust.edu.cn

© 2018 Chinese Physical Society and IOP Publishing Ltd

room-temperature powder x-ray diffraction (XRD) with Cu–Kα radiations (Bruker D8 Advance). Magnetic measurements were performed by using a physical property measurement system (PPMS, Quantum Design). Density-functional theory (DFT) calculations were performed to investigate the V position by using the general gradient approximation method (GGA) implemented in VASP code.[19] The plane-wave cut-off energy of 400 eV and high density of k grid of 19×19×19 points were used. In this study, we turned off the spin-orbit interaction and only considered the FM spin arrangements during the calculations.

3. Results and discussion

Figure 1 shows the room-temperature powder XRD patterns of $MnNi_{1-x}V_xGe$ ($x = 0.10$, 0.12, 0.14, 0.16 and 0.18) alloys. For the sample with $x = 0.10$, orthorhombic phase (TiNiSi-type structure, *Pnma*, space group 62) predominates. With increasing x to a value higher than 0.12, single hexagonal phase (Ni_2In-type structure, $P6_3/mmc$, space group 194) can be found. According to the XRD data, it can be concluded that the increase of V-content will reduce the T_t from 470 K, at which stoichiomtric MnNiGe alloy experiences the hexagonal-orthorhombic structural transformation,[20] to a value lower than room temperature. According to the XRD patterns, the lattice parameters of the samples with $x = 0.12$–0.18 are calculated. As is well known, the TiNiSi-type orthorhombic structure is an orthorhombic distortion of the Ni_2In-type hexagonal structure and the reduction of c_H/a_H ratio tends to stabilize the hexagonal structure. As listed in Table 1, with the increase of x, the values of c_H/a_H decrease gradually. It further reveals the decrease of T_t.

Table 1. Lattice parameters of the samples with $x = 0.12$–0.18.

samples	a_H	c_H	c_H/a_H
$x = 0.12$	4.0958(8)	5.4112(0)	1.3211(6)
$x = 0.14$	4.0998(4)	5.4074(6)	1.3189(4)
$x = 0.16$	4.1003(9)	5.4062(5)	1.3184(9)
$x = 0.18$	4.0971(8)	5.3974(2)	1.3173(7)

In ordered Ni_2In-type hexagonal compounds, the atomic occupancy follows a basic rule that the element with more valence electrons preferentially occupies Ni site, while the element with less covalent electrons intends to occupy Mn site.[21] According to this, the V atoms should not occupy Ni sites, but intend to occupy Mn sites and simultaneously extrude the same number of Mn atoms to the vacant Ni sites. The corresponding chemical formula is therefore $(Mn_{1-x}V_x)(Mn_xNi_{1-x})Ge$ instead of $MnNi_{1-x}V_xGe$. The two possible V atomic occupancies are illustrated in Fig 2. To check the V position, DFT calculations are carried out. During the calculation, x is assumed to be 0.25 for simplicity. The obtained results show that the $(Mn_{1-x}V_x)(Mn_xNi_{1-x})Ge$ displays a lower free energy (−9437.1082 eV) than $MnNi_{1-x}V_xGe$ (−9086.0930 eV), indicating that the V atoms obey the atomic occupancy rule.

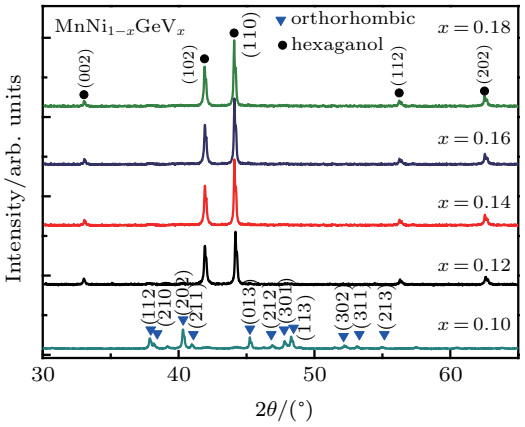


Fig. 1. (color online) Powder XRD patterns of $MnNi_{1-x}V_xGe$ ($x = 0.10$, 0.12, 0.14, 0.16 and 0.18) alloys at room temperature.

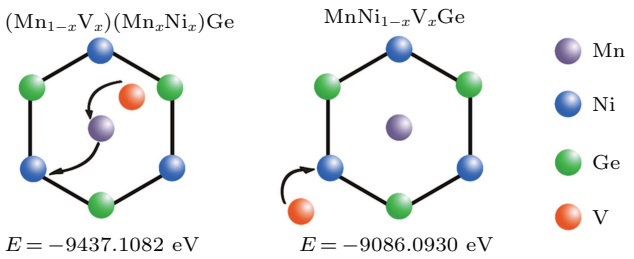


Fig. 2. (color online) Schematic diagrams of the two possible V atomic occupancies.

To investigate the magnetostructural coupling, the temperature dependences of magnetization (M–T) curves under a magnetic field of 5 T are shown in Fig. 3(a). The reason for us to choose such a high magnetic field is to overcome the influence of magnetocrystalline anisotropy on the measured magnetization so that the variation of saturated magnetization with V-content can be reflected in these M–T curves. In order to eliminate the potential virgin effect,[22] each sample is zero-field cooled to a temperature far below T_t prior to the measurement. The heating and cooling rate during measurement are both chosen to be 3 K/min. For the sample with $x = 0.10$, a continuous and reversible magnetic transition between FM and PM state is observed at ∼ 210 K. It indicates that this sample is stabilized at orthorhombic state and no structural transformation occurs below 400 K. With increasing x to 0.12, a sharp MST between PM hexagonal and high-magnetization orthorhombic phases is obtained. The obvious hysteresis demonstrates the first-order nature of the structural transformation. Similar phenomena can also be found in the samples with $x = 0.14$ and 0.16. Further increasing x will eliminate the structure transformation, leading to a smooth magnetic transition of hexagonal phase at 340 K in the sample with $x = 0.18$.

Since the orthorhombic MnNiGe possesses a spiral AFM ground magnetic state, the observed high magnetization is challenged. Figure 3(b) shows the isothermal magnetization curves of the sample with $x = 0.12$ at 160, 180, 200, and 220 K. Each curve exhibits a slope changing with increasing magnetic field, and the critical field (see inset of Fig. 3(b)), at which the slope changes, increases from 0.217 to 0.283 T with the temperature decreasing from 220 to 160 K. This phenomenon is a typical behavior of the magnetic-field-induced metamagnetic transition from AFM to FM state in MnNiGe-based alloy.[23–25] It should be noted that the critical magnetic field in stoichiometric MnNiGe is as large as 10 T. Therefore, V-doping greatly reduces the critical field. With further increasing x, the metamagnetic transition disappears and the sample with $x = 0.14$ exhibits FM behavior (Fig. 3(c)).

In MnMX alloys, since the Mn atoms are relatively isolated, magnetic moment is mainly localized on the Mn atoms.[21,26] The arrangement of Mn moments in orthorhombic phase is extremely sensitive to the nearest Mn–Mn separation.[27] Large Mn–Mn separation stabilizes ferromagnetic coupling while a small one leads to a spiral AFM state.[18] As mentioned above, the V atoms occupy the Mn sites. The large atomic radius of V atom will intend to increase the Mn–Mn separation after the structural transformation, and thus leading to ferromagnetic coupling between two Mn atoms. Therefore, the appearance of ferromagnetic state can be attributed to the increased Mn–Mn separation induced by V doping. Opposite case appears in $Mn_{1-x}Ni_{1+x}Ge$ alloys, in which Mn atoms are replaced by smaller Ni atoms so that AFM state is maintained.[28] On the other hand, as a nonmagnetic element, V atom cannot play the same role as Fe or Co atom, which can activate Fe–Mn or Co–Mn ferromagnetic coupling. However, the introduced V atoms can enlarge Mn–Mn separation, which also leads to local ferromagnetic coupling.

According to the M–T curves, the phase diagram of V-doped MnNiGe is obtained. As shown in Fig. 3(d), MST between FM orthorhombic and PM hexagonal phase can be established in a temperature region of 130 K, which ranges from $T_{C,H}$ (210 K) to $T_{C,O}$ (340 K). The width of this temperature region in which MST can be obtained is comparable to those of some other MnMX alloys, such as MnNiGe–CoNiGe system,[14] MnNiGe:Fe system,[16] and (Mn, Fe)Ni(Ge, Si) alloy.[29] In our system, the values of $T_{C,H}$ and $T_{C,O}$ are almost the same as that in orthorhombic MnNiGe alloy, indicating that V-doping cannot influence the strength of magnetic exchange. In Fig. 3(d), $T_{C,H}$, $T_{C,O}$, and T_t in heating and cooling process are defined as temperatures, at which $|dM/dT|$ is maximum. The values of T_t in heating and cooling process of the samples with $x = 0.10$–0.18 are further listed in Table 2.

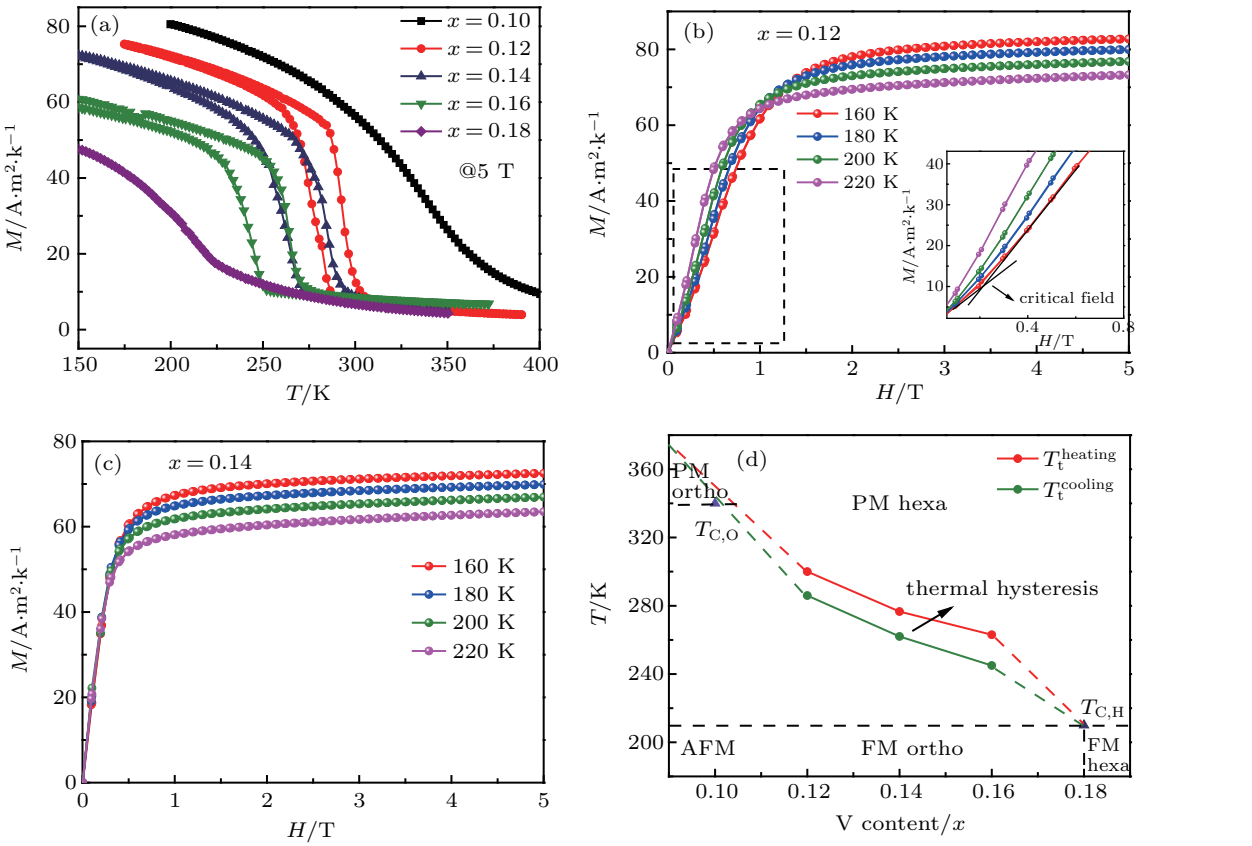


Fig. 3. (color online) (a) M–T curves of $MnNi_{1-x}V_xGe$ ($x = 0.10$, 0.12, 0.14, 0.16, and 0.18) alloys under 5 T. Isothermal magnetization curves of the sample with $x = 0.12$ (b) and (c) 0.14. (d) Phase diagram of V-doped MnNiGe alloys.

Table 2. Values of T_t in heating and cooling process of the samples with $x = 0.10$–0.18.

Samples	$T_t^{cooling}$/K	$T_t^{heating}$/K
$x = 0.10$	388.9[a]	420.5[a]
$x = 0.12$	280.4	293.6
$x = 0.14$	262.7	283.6
$x = 0.16$	241.3	264.1
$x = 0.18$	–	–

[a]measured by differential scanning calorimetry (DSC).

Due to the large Δ M between FM orthorhombic and PM hexagonal phase, the MST can be triggered by the magnetic field when the temperature is close to T_t. Figure 4(a) shows the M–T curves for the sample with $x = 0.12$ under magnetic fields of 0.1 (blue) and 5 T (orange). The hysteretic MST obviously shifts to the right with the increase of magnetic field, indicating that the MST can be induced by applying magnetic field. Additionally, it can be found that the low-field magnetization of orthorhombic phase increases with increasing the temperature. This behavior is due to the fact that reducing temperature will enlarge the critical field needed to drive the metamagnetic transition from AFM to FM state.

The magnetic-field-induced MST is always accompanied by considerable ΔS_m, which is highly related to the orthorhombic phase volume change during applying magnetic field.[17,30] Here, we use a method, instead of Maxwell relation which is thought to be inapplicable in the calculation of ΔS_m from a first-order transition, to estimate the ΔS_m based on calculating transformation volume fraction.[31] First, the M–T curve for the sample with $x = 0.12$ during heating is normalized. Then, the obtained curves are differentiated and fitted by using the following Gaussian equation:

$$v(T,H) = \frac{1}{\sigma\sqrt{\pi}} \cdot \exp\left[-\frac{(T-T_t)^2}{2\sigma^2}\right], \quad (1)$$

where σ indicates the transition width. The values of σ and T_t are 5.5 and 265 K under 0.1 T, while they change to 8.0 and 270 K with increasing the magnetic field to 5 T. The obtained results are shown in Fig. 4(a) (dark green and pink curves). Since the nucleation of martensite is random, the transition distribution function $v(T,H)$ is reasonable to follow Gaussian distribution. Based on this, the volume fraction of hexagonal phase at a given temperature T and magnetic field H can be obtained by integrating $v(T,H)$ from 0 to T K. Therefore, the magnetic-field-induced volume fraction increase (ΔV) of orthorhombic phase can be obtained from

$$\Delta V = \int_0^T v(T,\text{Low}-\text{field})\,\mathrm{d}T - \int_0^T v(T,\text{High}-\text{field})\,\mathrm{d}T. \quad (2)$$

Figure 4(b) shows the curve of calculated ΔV vs temperature with a magnetic field variation of 0 T–5 T (red curve). A maximum value of 33.4% can be obtained at ~ 270 K. According to ΔV, the ΔS_m can be calculated from $\Delta S_m = \Delta V \cdot \Delta S_{tot}$, where ΔS_{tot} is the total entropy change during the complete structural transformation from hexagonal to orthorhombic phase. The value of ΔS_{tot} can be obtained according to Clausius–Clapeyron relation ($\Delta S_{tot} = (\mathrm{d}B/\mathrm{d}T)\Delta M$).[32] For the sample with $x = 0.12$, the calculated maxium value of ΔS_{tot} is 45.08 J·kg^{-1}·K^{-1}, where $\Delta M = 46$ A·m^2·kg^{-1}, $\Delta B = 4.9$ T, and $\Delta T = 5$ K (Fig. 4(a)). Therefore, the temperature dependence of ΔS_m is obtained as shown in Fig. 4(b) (blue dotted curve). The maximum value is 15.057 J·kg^{-1}·K^{-1}. This value is comparable to those of some other magnetostructural transformation materials, such as $Ni_{50}Mn_{36}Sb_{14}$ (~ 5.2 J·kg^{-1}·K^{-1} at 0 T–5 T)[33] and $Ni_{50}Mn_{36}Ga_{29.6}$ (6 J·kg^{-1}·K^{-1} at 0 T–5 T)[34] alloys. Besides the entropy change, the refrigeration capacity (RC), which is calculated by numerically integrating the area under the ΔS_m–T curves through using the temperatures at half-maximum of the peak as the integration limits, is also important for estimating the magnetic cooling capacity.[35] The value of RC under the field of 0 T–5 T is 55.44 J·kg^{-1}, which is comparable to those in the other magnetocaloric materials, such as $Ni_{47}Co_2Mn_{39}Sn_{12}$ (23.36 J·kg^{-1} at 0 T–5 T)[36] and $Ni_{42}Mn_{47}Sn_{10}V$ (37.21 J·kg^{-1} at 0 T–5 T).[37] Furthermore, the observed thermal hysteresis is as large as 13.2 K. It will cause the functional degradation of MCE under magnetic cycles.[38,39] Therefore, how to reduce the thermal hysteresis in MnMX alloys is still a notable problem.

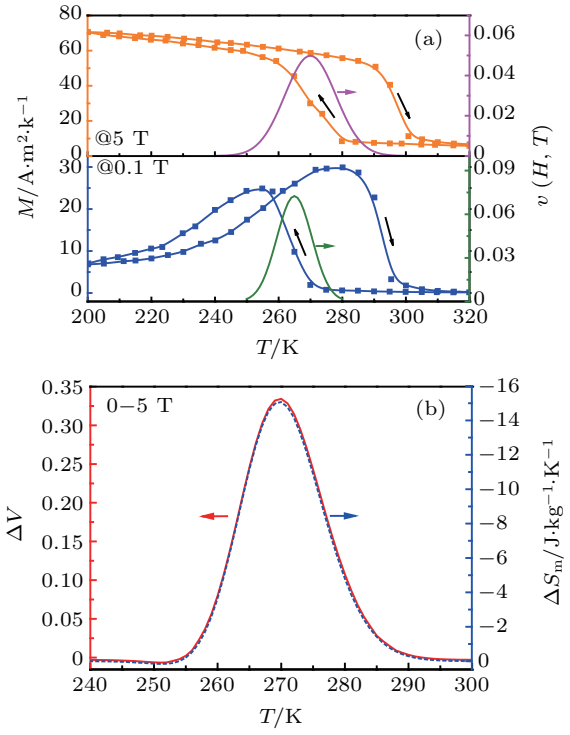


Fig. 4. (color online) (a) M–T curves for sample with $x = 0.12$ under magnetic fields of 0.1 (blue) and 5 T (orange). Dark green and pink curves are for fitted $v(T,H)$ curves. (b) Red curve denotes ΔV vs temperature with magnetic field variation of 0–5 T. Blue dotted curve refers to temperature dependence of ΔS_m with the magnetic field variation of 0–5 T.

4. Conclusions

In this work, the ferromagnetism and MST between PM hexagonal and FM orthorhombic phase are achieved in non-magnetic V-doped MnNiGe alloys. V atoms intend to occupy Mn sites and simultaneously extrude the same number of Mn atoms to the vacant Ni sites. It enlarges the Mn–Mn separation in orthorhombic phases, which further induces the ferromagnetic coupling between Mn moments. The V-doping also reduces the T_t into a temperature region between $T_{C,O}$ and $T_{C,H}$ so that PM–FM MST is established. The MST can be induced by the magnetic field, leading to considerable MCE.

References

[1] Kainuma R, Imano Y, Ito W, Sutou Y, Morito H, Okamoto S, Kitakami O, Oikawa K, Fujita A, Kanomata T and Ishida K 2006 *Nature* **439** 957
[2] Dutta P, Pramanick S, Majumdar S, Das D and Chatterjee S 2015 *J. Magn. Magn. Mater.* **395** 312
[3] Morellon L, Stankiewicz J, García-Landa B, Algarabel P A and Ibarra M R 1998 *Appl. Phys. Lett.* **73** 3462
[4] Yu S Y, Liu Z H, Liu G D, Chen J L, Cao Z X, Wu G H, Zhang B and Zhang X X 2006 *Appl. Phys. Lett.* **89** 162503
[5] Zhang C L, Wang D H, Cao Q Q, Xuan H C, Ma S C and Du Y W 2010 *Chin. Phys. B* **19** 37501
[6] Pecharsky V K and Gschneidner K A Jr. 1997 *Phys. Rev. Lett.* **78** 4494
[7] Wada H and Tanabe Y 2001 *Appl. Phys. Lett.* **79** 3302
[8] Dutta P, Pramanick S, Singh V, Major D T, Das D and Chatterjee S 2016 *Phys. Rev. B* **93** 134408
[9] Koyama K, Sakai M, Kanomata T and Watanabe K 2004 *Jpn. J. Appl. Phys. Part 1* **43** 8036
[10] Gama S, Coelho A A, de Campos A, Carvalho A M, Gandra F C G, von Ranke P J and de Oliveira N A 2004 *Phys. Rev. Lett.* **93** 237202
[11] Zhang X X, Zhang B, Yu S Y, Liu Z H, Xu W J, Liu G D, Chen J L, Cao Z X and Wu G H 2007 *Phys. Rev. B* **76** 132403
[12] Bażela W, Szytuła A, Todorovć J, Tomkowicz Z and Zięba A 1976 *Phys. Status Solidi A* **38** 721
[13] Oikawa K, Ito W, Imano Y, Sutou Y, Kainuma R, Ishida K, Okamoto S and Kitakami O 2006 *Appl. Phys. Lett.* **88** 122507
[14] Yu S Y, Ma L, Liu G D, Liu Z H, Chen J L, Cao Z X, Wu G H, Zhang B and Zhang X X 2007 *Appl. Phys. Lett.* **90** 242501
[15] Liu E K, Zhang H G, Xu G Z, Zhang X M, Ma R S, Wang W H, Chen J L, Zhang H W, Wu G H, Feng L and Zhang X X 2013 *Appl. Phys. Lett.* **102** 122405
[16] Liu E K, Wang W H, Feng L, Zhu W, Li G J, Chen J L, Zhang H W, Wu G H, Jiang C B, Xu H B and de Boer F 2012 *Nat. Commun.* **3** 873
[17] Zhang C L, Wang D H, Cao Q Q, Ma S C, Xuan H C and Du Y W 2010 *J. Phys. D* **43** 205003
[18] Zhang C L, Wang D H, Chen J, Wang T Z, Xie G X and Zhu C 2011 *Chin. Phys. B* **20** 097501
[19] Kresse G and Furthmüller J 1996 *Phys. Rev. B* **54** 11169
[20] Oikawa K, Ito W, Imano Y, Sutou Y, Kainuma R, Ishida K, Okamoto S and Kitakami O 2006 *Appl. Phys. Lett.* **88** 122507
[21] Szytuła A, Pedziwiatr A T, Tomkowicz Z and Bażela W 1981 *J. Magn. Magn. Mater.* **25** 176
[22] Zhang C L, Shi H F, Nie Y G, Ye E J, Han Z D and Wang D H 2014 *Appl. Phys. Lett.* **105** 242403
[23] Daniel-Pérez G, Sánchez Llamazares J L, Quintana-Nedelcos A, Álvarez-Alonso P, Varga R and Chernenko V 2014 *J. Appl. Phys.* **115** 17A920
[24] Jaworska-Gołąb T, Baran S, Duraj R, Marzec M, Dyakonov V, Sivachenko A, Tyvanchuk Y, Szymczak H and Szytuła A 2015 *J. Magn. Magn. Mater.* **385** 1
[25] Quetz, A, Samanta T, Dubenko I, Kangas M J, Chan J Y, Stadler S and Ali N 2013 *J. Appl. Phys.* **114** 153909
[26] Kaprzyk S and Nizioł S 1990 *J. Magn. Magn. Mater.* **87** 267
[27] Barcza A, Gercsi Z, Knight K S and Sandeman K G 2010 *Phys. Rev. Lett.* **104** 247202
[28] Zhang C L, Zhu C, Chen J, Wang T Z and Han Z D 2012 *J. Appl. Phys.* **112** 123911
[29] Wei Z Y, Liu E K, Li Y, Xu G Z, Zhang X M, Liu G D, Xi X K, Zhang H W, Wang W H, Wu G H and Zhang X X 2015 *Adv. Electron. Mater.* **1** 1500076
[30] Xu K, Li Z, Liu E, Zhou H, Zhang Y and Jing C 2017 *Sci. Rep.* **7** 41675
[31] Qu Y H, Cong D H, Sun X M, Nie Z H, Gui W Y, Li R G, Ren Y and Wang Y D 2017 *Acta Mater.* **134** 236
[32] Kainuma R, Imano Y, Ito W, Sutou Y, Morito H, Okamoto S, Kitakami O, Oikawa K, Fujita A, Kanomata T and Ishida K 2006 *Nature* **439** 957
[33] Du J, Zheng Q, Ren W J, Feng W J, Liu X G and Zhang Z D 2007 *J. Phys. D* **40** 5523
[34] Hu F X, Sun J R, Wu G H and Shen B G 2001 *J. Appl. Phys.* **90** 5216
[35] Zhang C L, Wang D H, Chen J, Wang T Z, Xie G X and Zhu C 2011 *Chin. Phys. B* **20** 097501
[36] Shah I A, ul Hassan N, Rauf A, Liu J, Gong Y Y, Xu G Z and Xu F 2017 *Chin. Phys. B* **26** 097501
[37] ul Hassan N, Shah I A, Khan T, Liu J, Gong Y Y, Miao X F and Xu F 2018 *Chin. Phys. B* **27** 037504
[38] Provenzano V, Shapiro A J and Shull R D 2004 *Nature* **429** 853
[39] Liu J, Gottschall T, Skokov K P, Moore J D and Gutfleisch O 2012 *Nat. Mater.* **11** 620